

# Electronic Structure of Dimethylenecyclobutane-1,3-dione. Photoelectron Spectroscopic Investigation<sup>1</sup>

Marie-Claire Lasne and Jean-Louis Ripoll

Laboratoire de Chimie des Composés thioorganiques, UA 480, Université de Caen, 14032 Caen, France

Christophe Lafon, Danièle Gonbeau, and Geneviève Pfister-Guillouzo\*

Laboratoire de Physico-Chimie Moléculaire, UA 474, Institut Universitaire de Recherche Scientifique, 64000 Pau, France

Received April 15, 1986

The He I PE spectrum of the transient title compound has been obtained by using the variable-temperature photoelectron spectroscopy technique. Agreement between the CIPSI calculations and experimental ion-state energies is very good. The electronic structure of this molecule is characterized by a net circumannular interaction and strong polar effects.

## Introduction

Flash pyrolysis of double Diels-Alder adducts has been enabled us to isolate various reactive polyunsaturated compounds, in particular dimethylenecyclobutane-1,3-dione (**1a**), which was characterized by NMR and low-temperature IR spectroscopy.<sup>2</sup> In order to interpret the high reactivity of this molecule toward 1,3-dienes, its electronic characteristics were investigated with photoelectron spectroscopy in order to define the different interactions existing between the conjugated groups.

A large number of theoretical and experimental publications have dealt with the estimation of orbital interactions between  $\pi$  groups bound to small ring systems, but the rings generally bore only two groups. Thus, cyclobutane-1,3-dione (**2a**) and its tetramethyl derivative **2b** have been extensively studied. Swenson and Hoffmann,<sup>3</sup> using EHT and CNDO/2 calculations, were the first to show that nonbonding pairs in position 1,3 interacted via a through-bond interaction. The experimental verification of this interaction is seen in the photoelectron spectrum, where the first two bands, respectively associated with the ionization of  $n^+$  and  $n^-$  combinations of nonbonding pairs of oxygens, are separated by 0.7 eV.<sup>4</sup> The UV spectrum of **2b** has been interpreted by transannular interactions between the  $\pi^*$  orbitals of carbonyl groups.<sup>5</sup> Recently, Pasto and Chipman<sup>6</sup> proposed a qualitative evaluation of these interactions: in agreement with Rao,<sup>7</sup> they concluded on an interaction via a greater degree of binding for the out-of-phase combination ( $b_{1g}$ ), associated with the band at 8.8 eV, than for the in-phase combination ( $b_{2u}$ ) associated with the band at 9.53 eV.

The interpretation is unambiguous in the case of 1,3-dimethylenecyclobutane (**3**).<sup>8</sup> A circumannular interaction

is observed between exocyclic  $\pi$  groups and the  $CH_2$  orbitals with  $\pi$  symmetry for the symmetrical combination associated with the 9.09-eV photoelectron band; the antisymmetric combination is associated with the 9.99-eV band.

## Experimental Section

Photoelectron spectra were recorded with a Helectros 0078 spectrometer. All spectra were calibrated with the  $^2P_{3/2}$  and  $^2P_{1/2}$  bands of xenon (12.13 and 12.43 eV) and of argon (15.76 and 15.93 eV). Thermolysis was at 700 °C directly in the ionization chamber, with a probe developed by LTD Laboratories.

Three thousand point spectra were acquired in 60 s with a 12-bit A/D converter board connecting the spectrometer to a micro-computer.

The difference in spectra was based on the simple criterion of avoiding negative counts in the 8.5–11-eV region.

SCF ground-state calculations were performed with the MONSTERGAUSS program.<sup>9</sup> A double- $\zeta$  quality 4-31G ab initio basis set was adopted.<sup>10</sup> This basis set was used to optimize all geometric parameters by a minimization process with variable metric, with gradient evaluation (Broyden-Fletcher-Goldfarb-Shanno algorithm).

The Foster Boys localization process<sup>11</sup> was used, generating localized  $\lambda_j$  orbitals (LMO). The examination of off-diagonal elements of the  $F_\lambda$  matrix enables through-space interactions to be characterized. In order to evaluate through-bond interactions between two LMO,  $\lambda_a$  and  $\lambda_b$ , it is possible to set the  $F_\gamma$  matrix to a partially diagonal  $F_\psi$  form and to carry out an examination of the off-diagonal elements of this matrix. The following three steps were used to obtain this matrix: (1) annihilation of off-diagonal elements in the  $F_\lambda$  matrix associated with rows and columns a and b; (2) diagonalization of the matrix, leading to a set of precanonical molecular orbitals (PCMO)  $\psi = P\lambda$ ; (3) expression of  $F_\gamma$  in the basis set of  $\psi F_\lambda \rightarrow F_\psi = PF_\lambda P^T$  (obtaining off-diagonal elements linking the PCMO  $\psi_a, \psi_b$  ( $\lambda_a$  and  $\lambda_b$  combinations) to the PCMO  $\psi_j$  ( $j \neq a', b'$ ), called relay orbitals).

In light of the size of the system, we were led to use a method of pseudo potentials<sup>12</sup> (PS HONDO program<sup>13</sup>) for the rigorous calculation of ionization potentials. The pseudo potentials and the double- $\zeta$  quality basis set (type 4-31G) previously determined<sup>14</sup> were adopted.

(1) Part 28: Application of Photoelectron Spectroscopy to Molecular Properties. Part 27: Guimon, C.; Pfister-Guillouzo, G.; Besancon, J.; Meunier, P. *J. Chem. Soc. Dalton Trans.*, in press.

(2) Ripoll, J. L.; Lasne, M. C. *Tetrahedron Lett.* 1978, 5201. Lasne, M. C.; Ripoll, J. L.; Denis, J. M. *Tetrahedron* 1981, 37, 503.

(3) Swenson, J. R.; Hoffmann, R. *Helv. Chim. Acta* 1970, 53, 2331.

(4) Corvan, O. D.; Gleiter, R.; Hashmall, J. A.; Heilbronner, E.; Hornung, V. *Angew. Chem., Int. Ed. Engl.* 1971, 10, 401. Dougherty, D.; Brint, P.; McGlynn, S. P. *J. Am. Chem. Soc.* 1978, 100, 5597.

(5) Koli, A.; McClary, E. *J. Ind. Chem. Soc.* 1978, 55, 242. Spafford, R.; Baiardo, J.; Wrobel, J.; Vala, M. *J. Am. Chem. Soc.* 1976, 98, 5217. Baiardo, J.; Spafford, R.; Vala, M. *J. Am. Chem. Soc.* 1976, 98, 5225.

(6) Pasto, D. J.; Chipman, D. M.; Worman, J. J. *J. Phys. Chem.* 1982, 86, 3981. Pasto, D. J.; Chipman, D. M.; Huang, N. Z. *J. Phys. Chem.* 1982, 86, 3990.

(7) Basu, P. K.; Chandra, Singh, U.; Tantry, K. N.; Ramamurthy, V.; Rao, C. N. R. *J. Mol. Struct. Theochem.* 1981, 76, 237.

(8) Hemmersbach, P.; Klessinger, M.; Bruchmann, P. *J. Am. Chem. Soc.* 1978, 100, 6344.

(9) Peterson, M.; Poirier, R. University of Toronto, Toronto, Ontario, Canada. Davidson, W. C.; Nazareth, L. *Argonne Natl. Techn. Nemos*, 303, 306, Argonne, IL.

(10) Ditchfield, R.; Hehre, W. J.; Pople, J. A. *J. Chem. Phys.* 1971, 54, 724.

(11) Foster, J. M.; Boys, S. F. *Rev. Mod. Phys.* 1960, 32, 300.

(12) Durand, P.; Barthelat, J. C. *Theor. Chim. Acta* 1975, 38, 283. Barthelat, J. C.; Durand, P. *Gazz. Chim. Ital.* 1978, 108, 225.

(13) Dupuis, M.; Rys, J.; King, J. F. *J. Chem. Phys.* 1976, 65, 111.

(14) Laboratoire de Physique Quantique, Toulouse, Ateliers, October 1981.

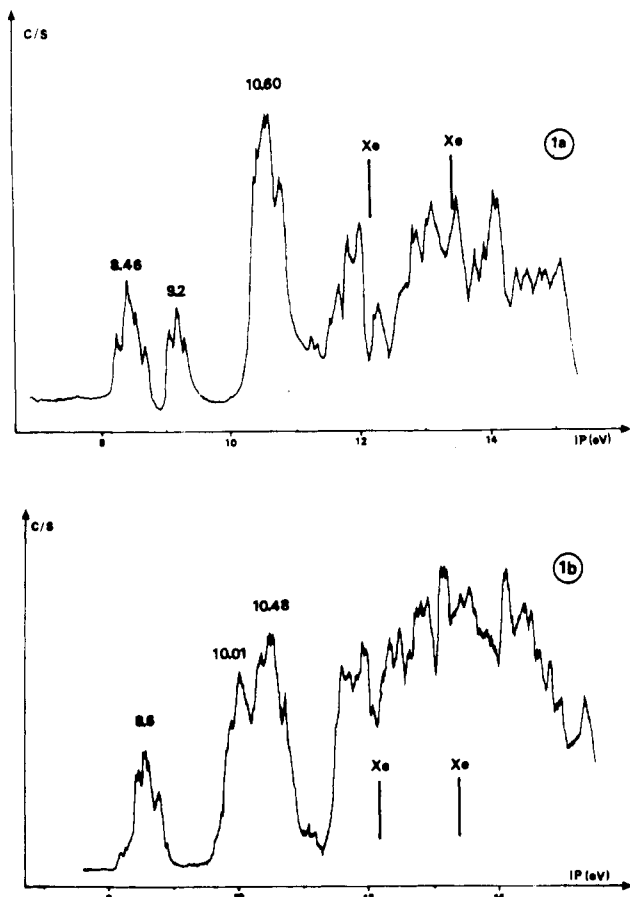
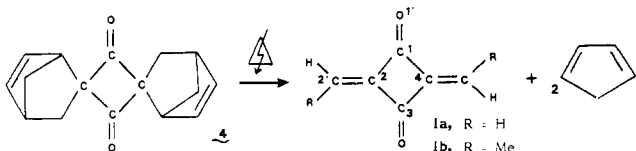


Figure 1. Photoelectron spectrum of (a) dimethylene-1,3-cyclobutanedione (1a) and (b) diethylidene-1,3-cyclobutanedione (1b).

The rigorous determination of the energies of ionic states required the use of the CIPSI<sup>15</sup> algorithm. A zero-order variation function was constructed by the iterative selection of the most important determinants the others were included through Møller-Plesset second-order perturbation. At the level of the variation function, 25 to 55 determinants were included,  $4 \cdot 10^6$  to  $9 \cdot 10^6$  thus being created by the perturbational treatment (a configuration interaction was also carried out at the level of the ground state).

**Photoelectron Spectra.** Flash pyrolysis of dispirocyclobutanedione 4 was carried out directly in the ionization chamber.



The spectrum obtained after subtracting cyclopentadiene ionizations is shown in Figure 1. The same figure shows the spectrum of diethylidene-1,3-cyclobutanedione (1b) recorded in the same way.

In this type of system, the ionization potentials observed between 9 and 11 eV are associated with the ionization of nonbonding pairs of oxygens in the ketone groups and the  $\pi$  electrons, especially those of the exocyclic ethylene bonds. The nature of the ionized molecular orbitals results from the degree of the through-space (1-2 and 1-3) and through-bond interactions.

Using a quantum chemical approach, we initially determined the geometric structure of this molecule in order to evaluate modifications of the cyclobutane skeleton. Interactions between groups were quantitatively defined by reformulating the

Table I. Orbital Energies of Dimethylene-1,3-cyclobutanedione (1a), 1,3-Cyclobutanedione (2a), and 1,3-Dimethylenecyclobutane (3)

compd 1a		compd 2a		compd 3	
$b_{1u}(\pi^+_{C=O})$	-16.56			$b_{1u}(\pi^+_{CH_2})$	-16.68
$b_{1g}$	-16.19			$b_{3u}$	-15.80
$b_{3u}$	-15.50			$b_{2g}(\pi^-_{CH_2})$	-14.70
		$b_{2g}(\pi^-_{C=O})$	-14.92	$b_{2u}$	-13.78
$b_{2g}(\pi^-_{C=O})$	-14.59	$b_{1u}(\pi^+_{C=O})$	-13.58	$b_{1g}$	-12.31
$b_{2u}(n^+_O)$	-12.71	$b_{2u}(n^+_O)$	-12.22	$b_{3u}$	-12.20
$b_{1u}(\pi^+_{C=C})$	-11.25	$b_{1g}(n^-_O)$	-11.11	$b_{3g}(\pi^-_{C=C})$	-10.11
$b_{3g}(\pi^-_{C=C})$	-11.18				
$b_{1g}(n^-_O)$	-10.75				
		$b_{1u}(\pi^{*+}_{C=C})$	2.42		
$b_{1u}(\pi^{*+}_{C=C})$	0.35	$b_{2g}(\pi^{*+}_{C=O})$	4.31	$b_{1u}(\pi^+_{C=C})$	-9.18
$b_{2g}(\pi^{*+}_{C=O})$	4.35			$b_{1u}(\pi^{*+}_{C=C})$	4.10
$b_{3g}(\pi^{*+}_{C=C})$	4.61				

through-space and through-bond interaction diagrams on the basis of localized orbitals.<sup>16</sup> Using this minimized structure, we subsequently carried out a rigorous calculation of the first four ionic states. The aim of this procedure was to verify the coherence between experimental and quantum chemical data and to assure the reliability of our conclusions on the nature of the interactions occurring.

### Quantum Chemical Calculations: Ground State

**Geometric Parameters.** Figure 2 lists all the minimized geometric parameters of 1a. For the sake of comparison, we have also included those obtained for compounds 2a and 3. The calculated geometries of 2a and the experimental structure of 2b obtained by X-ray diffraction<sup>17</sup> are in particularly satisfying agreement. See the paragraph at the end of paper about supplementary material.

In comparison to cyclobutane-1,3-dione (2a) and 1,3-dimethylenecyclobutane (3), there is a shortening of the C-C bond of the ring to a value identical with that of bis[2,4-(diphenylmethylene)]cyclobutane-1,3-dione<sup>18</sup> (1.498 Å). In addition, the C<sub>1</sub>-C<sub>3</sub> and C<sub>2</sub>-C<sub>4</sub> bond lengths, 2.11 and 2.12 Å, are on the same order as those observed for 2a and 3 (2.10 Å and 2.12 Å). The transannular interactions observed for these systems can be expected to have the same importance for 1a. The exocyclic ethylene double bond is 1.31 Å long and the ring angles are very close to 90°.

**Molecular Orbitals.** Table I shows energy levels listed as a function of symmetry, choosing the z axis as the axis of highest symmetry and the x axis along the C=O bonds.

The energies of the orbitals of 1a corresponding to the nonbonding pairs  $n_O$  are -10.75 and -12.71 eV, i.e., a 2-eV separation. This separation is only 1 eV in 2a. An  $n^+$  orbital with  $b_{2u}$  symmetry is noted for these two molecules with deeper energy than the  $n^-$  orbital with  $b_{1g}$  symmetry.

In the case of dimethylenecyclobutanedione and in contrast to cyclobutanedione, this  $b_{2u}$  orbital presents a  $\sigma_{C=C}$  exocyclic bond character and a slight localization on carbons C<sub>1</sub> and C<sub>3</sub>. This apparently indicates a slight through-bond interaction for the  $n^+$  combination. The interaction for the  $b_{1g}$  combination, on the other hand, occurs via the orbital with the same symmetry as the cyclobutane ring and appears to be greater, with notable localization on the C<sub>1</sub> and C<sub>3</sub> atoms.

This difference in through-bond interaction appears in the wave function contours of the  $b_{1g}$  and  $b_{2u}$  orbitals

(15) Huron, B.; Malrieu, J. P.; Rancurel, P. *J. Chem. Phys.* 1973, 58, 5745. Pelissier, M. Thèse, Université Paul Sabatier, Toulouse, France, 1980.

(16) Heilbronner, E.; Schmelzer, A. *Helv. Chim. Acta* 1979, 58, 936.

(17) Shirrel, C. D.; Williams, D. E. *Acta Crystallogr., Sect. B: Struct. Sci.* 1974, 30, 245.

(18) Gatehouse, B. M. *Cryst. Struct. Commun.* 1982, 11, 369.

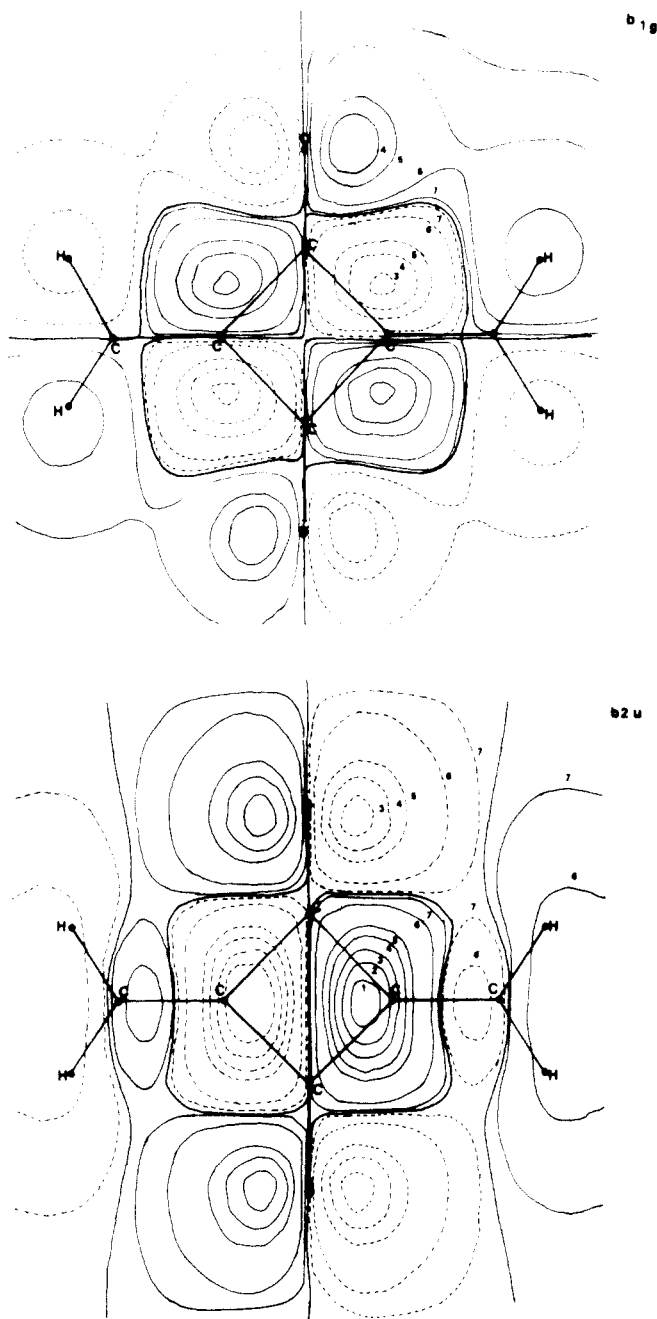


**Figure 3.** Wave function contours: orbitals  $b_{1g}$  and  $b_{2u}$ . Contour values 1, 2, 3, 4, 5, 6, 7 are equal to 0.35, 0.3, 0.25, 0.2, 0.15, 0.05, 0.01 (electron Bohr<sup>-3</sup>)<sup>1/2</sup>.

(Figure 3). The latter exhibits a clearly greater localization on the oxygen atoms.

One of the characteristics of this system is the importance of interactions between  $\pi$  orbitals and especially the energy position of the exocyclic ethylene system. In comparison to dimethylenecyclobutane **3**, the circumannular interaction occurs via the ketone groups. There is relatively weak overlapping between  $\pi_{C=C}$  and  $\pi_{C=O}$ . The SCF energies of the antisymmetric and symmetric combinations of  $\pi_{C=C}$  are very close, in the order  $b_{1u} < b_{3g}$ . The transannular interaction between the two ethylene groups thus appears to be compensated by the circumannular  $\pi_{C=C}-\pi_{C=O}$  interaction. The latter interaction, however, appears to be greater at the level of virtual orbitals (greater localization on the ring carbons in  $\pi^*_{C=O}$ ), since a vacant  $b_{1u}$  orbital is observed in this system with a particularly low energy (+0.35 eV). The energy position of this vacant orbital is probably the basis of the very high reactivity of

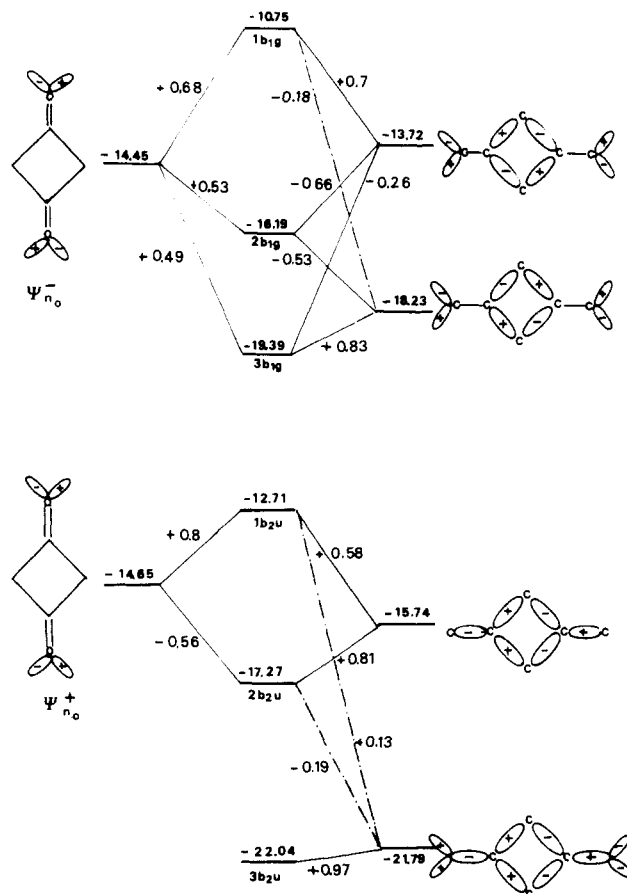


**Figure 4.** (a) Interactions between  $\psi^-_{n_0}$  and the relay orbitals of  $b_{1g}$  symmetry. (b) Interactions between  $\psi^+_{n_0}$  and the relay orbitals of  $b_{2u}$  symmetry.

this compound towards 1,3-dienes.

**Interactions of Localized Orbitals.** In order to quantitatively estimate the importance of the interactions occurring, we reformulated the interaction diagrams on the basis of localized orbitals.

**Nonbonding Pairs of Oxygen Atoms.** As can be expected, through-space interaction is practically nil. Figure 4 shows the interactions between  $\psi^-_{n_0}$  and  $\psi^+_{n_0}$  and the relay orbitals, leading to canonical molecular orbitals  $b_{1g}$  and  $b_{2u}$ . For the two antisymmetric and symmetric combinations, we initially note strong through-bond interactions: 3.70 eV ( $\epsilon_{b_{1g}} - \epsilon_{\psi^-_{n_0}}$ ) and 1.95 eV ( $\epsilon_{b_{2u}} - \epsilon_{\psi^+_{n_0}}$ ).

At the level of the  $\psi^-_{n_0}$  combination, we observe primarily the interaction of the relay characteristic of the  $b_{1g}$  orbital of cyclobutane and the antisymmetric combinations of the C-H bonds. The lesser destabilization of the  $\psi^+_{n_0}$  combination results from an interaction with the relays characteristic of the  $b_{2u}$  orbital of cyclobutane and the exocyclic C-C bonds. The energy of this relay is initially lower and presents above all a lesser localization on the cyclobutane orbitals, implying a lower degree of overlap with the nonbonding pairs of oxygen.

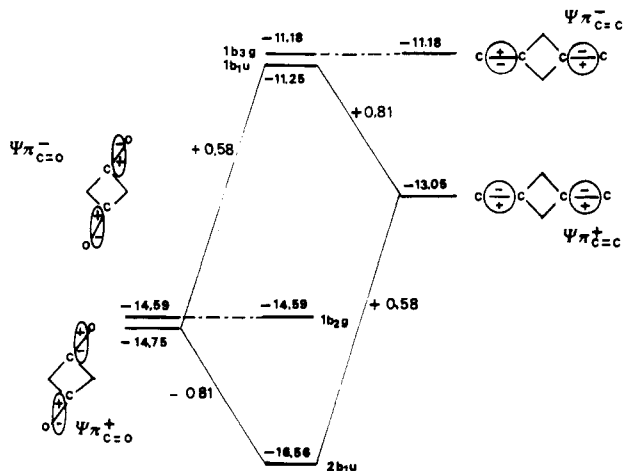
Though-bond interaction is thus much greater for the  $b_{1g}$  combination and in general we observe more mixing between this orbital and the two relay orbitals of the same symmetry.

In the case of the  $b_{2u}$  orbital, these interactions result in a greater localization on the nonbonding pairs, through-bond interactions occurring only via a single relay orbital. The system in this symmetry group remains much more localized.

**$\pi$  System.** We initially note a greater transannular interaction between the  $\pi_{C=C}$  bonds ( $\Delta\epsilon = 1.87$  eV) than

Table III. Calculated Ionization Potentials (eV)

state	Koopman PS HONDO	polarization	pair correlation	corrected, IP	diagonalized polarization	correlation of ion	calcd IP CIPSI	expl IP
${}^2B_{1g}$	10.86	-1.14	+0.13	9.85	-0.94	-1.35	8.41	8.46
${}^2B_{2u}$	12.83	-1.31	+0.11	11.63	-1.02	-1.9	9.61	9.25
${}^2B_{1u}$	11.32	-0.6	+0.23	10.95			10.58	10.60
${}^2B_{3g}$	11.25	-1	+0.31	10.56			10.72	
${}^4B_{1g}$ (monoexcitation $b_{1u}^* \leftarrow b_{1u}$ for ionic state ${}^2B_{1g}$ )							11.31	
								11-11.3
${}^2B_{1g}$							11.55	
${}^4B_{2u}$ (monoexcitation $b_{2g}^* \leftarrow b_{1u}$ for ionic state ${}^2B_{1g}$ )							12.13	
${}^2B_{2u}$							12.65	

Figure 5. Orbital energies after interaction of the PCMO  $b_{3g}$  and  $b_{1u}$ .

between the  $\pi_{C=C}$  bonds ( $\Delta\epsilon = 0.16$  eV). The importance of these transannular interactions is also shown by the Mulliken overlap population indexes, respectively calculated to be  $-0.43$  and  $-0.12$ .

The spatial interaction between the  $C=O$  and  $C=C$  groups is relatively important, since the symmetric  $\pi_{C=C}^+$  combination exhibits an interaction with the symmetric  $\pi_{C=O}^+$  combination, leading to a 1.8-eV destabilization. This circumannular interaction is about twice as great as the transannular interaction cited above. For the  $b_{1u}$  combination, this results in a clearcut delocalization on all the exocyclic  $\pi$  groups (Figure 5).

**Charge Diagram, Overlap Populations.** Table II lists the net charges,  $\pi$  charges, and the Mulliken population indexes. See the paragraph at the end of paper about supplementary material.

The most striking fact is the clearcut polarization of this system. The net total charges are respectively  $Q_{C_1} = +0.49$ ,  $Q_O = -0.56$ ,  $Q_{C_2} = -0.12$ ,  $Q_{C_3} = -0.25$ . In parallel to repulsive transannular interactions, notably between the two  $C=C$  bonds dipole-dipole interactions are important. The destabilizing interactions, spatial and through-bond analyzed above, are not a priori more important than for molecules 2 and 3. It thus seems that the origin of the thermodynamic instability of this system is in the strong polarity of the bonds inducing considerable polar interactions.

### Ionic States

The poor concordance between the calculated orbital energies and the experimental ionization potentials shows the impossibility of interpreting the photoelectron spec-

trum on the basis of the Koopmans' approximation. It is indispensable to take into account polarization and correlation effects for this molecule with nonbonding pairs and considerable conjugation.

We initially estimated polarization and pair correlation effects by using a partial perturbational procedure.<sup>19</sup> The estimated corrections, even considering an underestimation of the loss of correlation energy, do not correctly reflect the experimental spectrum. We thus carried out a complete perturbational procedure with the CIPSI algorithm. In order to define the importance of polarization and specific correlation effects of the ion, we also carried out a separate diagonalization of the configurations reflecting these two corrections in comparison to Koopmans.

The results (Table III) show a weak polarization effect for the ionization of the nonbonding pairs of oxygen, about 1 eV, which was also relatively well shown by the partial perturbational procedure. As a result of the presence of a low-energy  $\pi^*$  orbital, the correlation effect of the ion itself is very high at 1.35 eV for the  ${}^2B_{1g}$  state and 1.9 eV for the  ${}^2B_{2u}$  state. The loss of ground-state correlation is greater than that determined uniquely on the loss of pair correlation. An important factor with these delocalized systems is the fact the interpair correlation is not taken into account.

In the case of the two ionic  $\pi$  states, the greatest correction effect corresponds to the electronic reorganization of ionic states. This phenomenon is probably related to the high polarity of these bonds.

We also attempted to determine the energies of non-Koopmans ions of this highly conjugated molecule. We concentrated on the non-Koopmans ions of the first  ${}^2B_{1g}$  ionic state, corresponding to  $\pi^* \leftarrow \pi$  excitations. The energies of non-Koopmans configurations are much higher for the other ionic states, either  $\pi$  ionic states or the second  $\sigma$  ionic state. For the first ionic state, monoexcitation  $\pi^*b_{1u} \leftarrow \pi b_{1u}$  leads to a quadruplet state  ${}^4B_{1g}$  with an energy of 11.31 eV, one of the doublet states  ${}^2B_{1g}$  having an energy close to 11.55 eV. Similarly, for this same ionic state, the monoexcitation  $\pi^*b_{2g} \leftarrow \pi b_{1u}$  is associated with a quadruplet  ${}^4B_{2u}$  having an energy of 12.13 eV and a doublet  ${}^2B_{2u}$  at 12.65 eV. The non-Koopmans ions associated primarily with the  $\pi^*b_{3g} \leftarrow \pi b_{3g}$  excitation have a higher energy, although this configuration participates to a slight extent in the  ${}^4B_{1g}$  and  ${}^2B_{1g}$  states. As invoked in the case of polyunsaturated hydrocarbons<sup>20,21</sup> dimethylenecyclobutadione appears to furnish additional examples of low-

(19) Daudey, J., private communication. Gonbeau, D.; Pfister-Guilouzo, G. *J. Electron Spectrosc. Relat. Phenom.* 1984, 33, 279.

(20) Koenig, T.; Southworth, S. *J. Am. Chem. Soc.* 1977, 99, 2807.

(21) Kreile, J.; Munzel, N.; Schulz, R.; Schweig, A. *Chem. Phys. Lett.* 1984, 108, 609.

energy participation of non-Koopmans states.

Considering the above data, the experimental spectrum is satisfyingly interpreted. The first two bands observed at 8.46 and 9.2 eV are associated with the ionization of the  $b_{1g}$  and  $b_{2u}$  combinations of nonbonding pairs of oxygen. We note a similar intensity for these two bands.

As seen above, the  $b_{2u}$  orbital presents a clear localization on the ethylene carbons, explaining why the band is shifted toward lower energies after a monomethylation: a first broad band centered at 8.6 eV is observed, covering the two ionizations. The first band presents a clear vibrational structure of about  $1200\text{ cm}^{-1}$ , showing the slight geometric reorganization of the ion. In the case of the second less structured band, the vibrational space is lower, and, in addition to valence vibrations  $\nu_{C=O}$ , may correspond to vibrations associated with the  $\nu_{C=C}$  group. The third dimethylenecyclobutanedione band more intense at 10.60 eV corresponds to the  ${}^2B_{1u}$  and  ${}^2B_{3g}$  ionic states. The calculated energies are very close and the two bands overlap. After methylation, however, the  $B_{1u}$  state, more delocalized on C=O bonds, is associated with the band at 10.48 eV, while the  ${}^2B_{3g}$  state corresponds to the band at 10.01 eV.

In the 11 eV region of both spectra, there is a low-intensity band as a shoulder of the broad band of the non-substituted derivative and as a distinct band for the methylated derivative. This band is probably associated

with the non-Koopmans  ${}^4B_{1g}$  and  ${}^2B_{1g}$  states.

### Conclusion

The photoelectron spectrum of dimethylenecyclobutane-1,3-dione was obtained by using the technique of spectrometer-coupled flash pyrolysis. We show the participation of a low-energy shake-up structure for this compound. The excellent agreement between experimental results and theoretical predictions illustrates the usefulness of the CIPSI approach for the calculation of ionic states. The electronic structure of this molecule is characterized by a clear circumannular interaction, inducing a particularly low-energy position for the first vacant orbital, the basis of the high reactivity towards 1,3-dienes. Destabilizing through bond interactions, however, apparently cannot explain its instability, probably more related to polar effects.

**Acknowledgment.** The authors thank the Centre de Calcul Vectoriel pour la Recherche France for generous allotments of computer time (ATP Cray 1984).

**Registry No.** 1a, 71028-83-6; 1b, 78507-07-0; 2a, 15506-53-3; 3, 2045-78-5; 4, 71028-82-5.

**Supplementary Material Available:** Charges and overlap populations for 1a (Table II) and bond distances (Å) and angles calculated for 1a, 2a, and 3 (Figure 2) (1 page). Ordering information is given on any current masthead page.

## Reactivity Effects on Site Selectivity in Nucleoside Alkylation: A Model for the Factors Influencing the Sites of Carcinogen-Nucleic Acid Interactions

Robert C. Moschel,\* W. Robert Hudgins, and Anthony Dipple

*BRI-Basic Research Program, Laboratory of Chemical and Physical Carcinogenesis, NCI-Frederick Cancer Research Facility, Frederick, Maryland 21701*

Received July 9, 1986

Product distributions are described for 15 reactions between guanosine (1) and a series of *p*-Y-benzyl bromides (2a-e), *p*-Y-benzyl chlorides (3a-e), and *N*-nitroso-*N*-(*p*-Y-benzyl)ureas (4a-e) where Y = a, O<sub>2</sub>N; b, Cl; c, H; d, CH<sub>3</sub>; e, CH<sub>3</sub>O. The yields of products from reaction at the 7-position of guanosine to produce 7-(*p*-Y-benzyl)guanosines (5a-e), at N<sup>2</sup> to produce N<sup>2</sup>-(*p*-Y-benzyl)guanosines (6a-e), at the O<sup>6</sup>-position to produce O<sup>6</sup>-(*p*-Y-benzyl)guanosines (7a-e), and at the 5-position to produce 4-(*p*-Y-benzyl)-5-guanidino-1-β-D-ribofuranosylimidazoles (8a-e) are correlated with the mechanism of the reaction (i.e., the S<sub>N</sub>2 or S<sub>N</sub>1 character) imposed by the para substituent and/or leaving group and the nature of the incipient charge density (i.e., the "hardness" or "softness") at the reaction center. These observations, coupled with the literature on sites of reaction of carcinogens with nucleic acid components, are used to rationalize the site selectivity differences exhibited by the alkylating and aralkylating classes of carcinogens in their nucleic acid reactions.

Organic chemical carcinogens are electrophilic species that are either directly reactive from the outset or are produced by metabolism of a precarcinogenic and non-chemically reactive form.<sup>1-3</sup> Once these reactive species are produced, their rates, extents, and sites of reaction on cellular macromolecules, such as DNA, are governed by their intrinsic electrophilic reactivity. This reactivity leads to substitution at a variety of sites on the multidentate heterocyclic nucleic acid base components of DNA. For

example, the weakly carcinogenic alkylating agents (e.g., methyl methanesulfonate) primarily modify the pyridine-type ring nitrogen sites (e.g., the 7-position of guanine residues)<sup>4</sup> while the more potent carcinogenic alkylating agents (e.g., the *N*-alkyl-*N*-nitroso compounds) modify exocyclic oxygen centers (e.g., O<sup>6</sup> of guanine residues) in addition to ring nitrogen sites.<sup>5,6</sup> In contrast, the aralkylating 7-(bromomethyl)benz[*a*]anthracenes,<sup>7,8</sup> the di-

(1) Miller, E. C.; Miller, J. A. *Pharmacol. Rev.* 1966, 18, 805-838.  
 (2) Dipple, A.; Lawley, P. D.; Brookes, P. *Eur. J. Cancer* 1968, 4, 493-506.  
 (3) Miller, J. A.; Miller, E. C. *J. Natl. Cancer Inst.* 1971, 47, 5-14.

(4) Lawley, P. D. *Prog. Nucleic Acid Res. Mol. Biol.* 1966, 5, 89-131.  
 (5) Loveless, A. *Nature (London)* 1969, 223, 206-207.  
 (6) Singer, B. *Prog. Nucleic Acid Res. Mol. Biol.* 1975, 15, 219-332.  
 (7) Dipple, A.; Brookes, P.; Mackintosh, D. S.; Rayman, M. P. *Biochemistry* 1971, 10, 4323-4330.